# Dynamics of the water-catalyzed phototautomerization of 7-azaindole

**ARTICLE** *in* THE JOURNAL OF CHEMICAL PHYSICS · MAY 2001

Impact Factor: 2.95 · DOI: 10.1063/1.1361073

# Dynamics of the water-catalyzed phototautomerization of 7-azaindole

Antonio Fernández-Ramos, Zorka Smedarchina, Willem Siebrand,[a)]
and Marek Z. Zgierski
*Steacie Institute for Molecular Sciences, National Research Council of Canada, Ottawa, K1A 0R6 Canada*

(Received 15 August 2000; accepted 12 February 2001)

Multidimensional *ab initio* proton tunneling rate constants are reported for the tautomerization of singlet-excited 7-azaindole complexed with water, represented by discrete water molecules with and without a dielectric continuum. The results are compared with experimental observations in cold beams and in room-temperature aqueous solutions. For complexes with one and two water molecules, potential-energy surfaces are calculated at the complete active space multiconfiguration self-consistent-field [CASSCF(8,8)] level. For comparison with solution data, the structures are reoptimized inside a spherical cavity according to the Onsager model. To compare the effect of the dielectric with that of a secondary solvent shell, the structure of 1:1 and 1:2 complexes solvated by four and three additional water molecules so as to form 1:5 complexes, are optimized at the CASSCF(8,8) level with single-point Onsager corrections. Based on these potential-energy surfaces, temperature-dependent multidimensional proton transfer rate constants are calculated with a recently developed version of the instanton approach. It is found that in gas-phase 1:1 and 1:2 complexes tautomerization occurs through concerted double and triple proton transfer, respectively. The calculated low-temperature rate constants agree with the observation that in these complexes no tautomerization occurs within the fluorescence lifetime of about 8 ns. Addition of a dielectric continuum within the Onsager model cannot explain the room-temperature rate constant of about $10^{10}$ $s^{-1}$ observed as the fast tautomerization component of excited 7-azaindole in protic solutions. Addition of a secondary solvent shell of four water molecules to the 1:1 complex has only a minor effect on the proton transfer rate, but addition of a secondary shell of three water molecules to the cyclic 1:2 complex yields rate constants of the observed order of magnitude. This happens because the double bridge facilitates charge separation, which stabilizes an ion-pair structure for the transition state. As a result the barrier is lowered drastically and although the proton effective mass is also increased, the effect of the lower barrier dominates, leading to much faster proton transfer. It is concluded that the fast rate component observed in room-temperature tautomerization of excited 7-azaindole in water and alcohols corresponds to proton transfer through a bridge of two hydrogen-bonded water molecules, rather than through a single-molecule water bridge as previously assumed. The predicted mechanism involves a (meta)stable intermediate state.  [DOI: 10.1063/1.1361073]

## I. INTRODUCTION

Recently we reported calculations on the dynamics of tautomerization of guanine and 7-azaindole,[1] and of 3-hydroxyisoquinoline,[2] brought about by proton transfer through water bridges. In these examples, the bridges consisted of one or two water molecules and the corresponding transfer of two or three protons was concerted but not necessarily synchronous. Nonclassical synchronous transfer was predicted for bridges with equivalent hydrogen bonds, where the proton shifts will cause minimal displacement of the heavier atoms. If the protons move asynchronously, a transient charge separation is generated and the resulting force exerted on these atoms will tend to displace them. If there were no effect on the barrier height, this would slow down the reaction since it would increase the effective mass of the tunneling protons resulting from the reorganization of the heavy atoms. However, asynchronicity implies that not all hydrogen bonds are broken simultaneously, which will tend to result in a lower barrier. In the limiting case where the reaction decomposes into a multistep process, the barrier corresponds to the breaking of a single hydrogen bond plus the energetic penalty, if any, associated with charge separation. This penalty will be large in the gas phase but may be small or negligible in a strongly polar environment. The increasing effective mass and the decreasing barrier height associated with a loss of synchronicity affect the transfer rate in opposite ways. The balance between these two opposing effects will strongly depend on the nature of the solvent.

In this paper we explore the mechanism of proton transfer in singlet-excited 7-azaindole ($7AI/S_1$) in the presence of one, two, and five water molecules. We choose this example because experimental data have been reported indicating that this transfer exhibits a strong solvent dependence. Complexes of $7AI/S_1$ with water molecules have been studied in cold beams, the pertinent observation being that the 1:1 and

[a)]Electronic mail: willem.siebrand@nrc.ca

 

1:2 complexes show no tautomerization within the 8 ns lifetime of the fluorescence.[3–5] This observation implies that the zero-temperature tautomerization rate constant in the fluorescent state cannot be larger than about $10^7$ $s^{-1}$. On the other hand, it has been observed[6–10] that in solutions in water and alcohols, 7AI/$S_1$ tautomerizes in about $10^{-10}$ s. Based on such experiments it has been proposed[6–10] that this fast process is mediated by a bridge consisting of a single water molecule. Since the corresponding complex does not tautomerize in a cold beam, it follows that the combined effects of temperature and solvation would have to increase the proton transfer rate leading to tautomerization in the excited state by a factor of at least 1000.

Tautomerization of 7AI·water complexes involves exchange of light (H) atoms between pairs of heavier (N and O) atoms; therefore quantum-mechanical tunneling is expected to contribute significantly to the rate of reaction. To evaluate this rate as a function of temperature, we require a dynamics theory capable of dealing with multidimensional proton tunneling in relatively large systems. For this we choose the instanton approach in the form used in Refs. 1 and 2, which allows direct evaluation of the rate constant for the 1:1 and 1:2 complexes of 7AI/$S_1$. For the ground state of the 7AI complexes the tautomerization rate constant was found[1] to increase only by a factor of order 10 between 0 and 300 K. Such a weak temperature dependence at low temperatures is typical for concerted proton tunneling. Quantum-chemical calculations indicate that concerted multiproton transfer is also the prevailing mechanism in the excited gas-phase complexes of 7AI.[11–13] This suggests that the increase by factor of order 1000 or larger for the transfer rate in solution cannot be explained solely as a temperature effect, a suggestion supported by recently reported low-level calculations for the 1:1 complex[13] and by the higher-level calculations for both complexes reported below. Therefore we investigate the effect of solvation on the complexes in order to probe to what extent this will stabilize charge separation in transitional structures and to compare the expected opposing effects of lower barriers and higher effective masses resulting from the reorganization of the heavy atoms.

A simple method to study the effect of a bulk solvent is to place the complex in a cavity inside a dielectric medium. The effect on the potential energy is conveniently represented by the self-consistent reaction field as implemented in the Onsager model.[14] Although the method allows full geometry optimization, the cavity is spherical and hence does not accurately represent the shape of the molecule. Also, the effect of solvent molecules close to the complex cannot be mimicked realistically by a dielectric continuum. In an attempt to obtain a more realistic representation of the bulk solvent effect, we have considered models with additional water molecules. These will form a secondary solvent shell of molecules not directly hydrogen-bonded to 7AI. Since such large complexes are computationally demanding, we have looked for an arrangement where a limited number of water molecules will have a large effect. Based on the results for the 1:1 and 1:2 complexes as well as on a number of exploratory calculations, we choose for detailed investigation 1:5 clusters corresponding to 1:1 and 1:2 complexes microsolvated by four and three water molecules, respectively.

The calculations proceed in two stages. First we calculate the structure, energy and vibrational force field of the excited complexes to be investigated, using standard quantum-chemical code, in this case GAUSSIAN 98[15] and GAMESS.[16] Then we use these results as input parameters in a dynamics program suitable for multidimensional proton tunneling, for which we choose our own instanton method as implemented in the DOIT 1.2 code.[17] In the next section we present a brief outline of this method in the form used for the present calculations.

## II. THEORY

Since the dynamics approach is the same as that used for ground-state 7AI[1] and for 3-hydroxyisoquinoline[2] complexes, we limit ourselves here to a brief outline.

The instanton formalism is a multidimensional quasiclassical approach to tunneling rate phenomena based on the concept of least action. It can be applied to the dynamics of a system where the tunneling motion along the reaction coordinate $x$ is coupled to a number of vibrations $\mathbf{y}$, described by the Hamiltonian

$$H[x(\tau),\mathbf{y}(\tau)]=\tfrac{1}{2}\dot{x}^2+\tfrac{1}{2}\dot{\mathbf{y}}^2+U(x,\mathbf{y}). \tag{1}$$

Below a specific (crossover) temperature, there are periodic orbits with period equal $\beta=1/k_BT$, where the Euclidian action

$$S_E=\int_{-\beta\hbar/2}^{\beta\hbar/2} d\tau\, H[x(\tau),\mathbf{y}(\tau)] \tag{2}$$

defined in imaginary time $\tau=it$ has an extremal value. Two trivial solutions of the extreme value equations correspond to the (quasi)equilibrium configuration and the transition state, respectively, the latter being a saddle point. There is another extremal trajectory, called the instanton (bounce) path, which is also a saddle point. The two saddle points contribute to the imaginary part of the partition function, which in turn defines the rate constant of decay of the metastable state. The transition state contributes a term proportional to $e^{-U_0/k_BT}$, where $U_0$ is the barrier height, and the instanton a term proportional to $e^{-S_I(T)}$, where $S_I$ is the Euclidian action (in units $\hbar$) corresponding to the instanton path. The tunneling component of the rate constant is thus of the form

$$k_{\mathrm{tun}}(T)=A(T)e^{-S_I(T)}, \tag{3}$$

where the prefactor $A(T)$ represents the effect of trajectories adjacent to the instanton path. At temperatures approaching the crossover temperature, the instanton converges into the transition state and the rate then is that of an over-the-barrier transition. It can be evaluated by standard methods, e.g., by transition-state theory[18]

$$k_{\mathrm{cl}}(T)=\frac{k_BT}{h}\frac{Z^{TS}}{Z^R}e^{-U_0/k_BT}, \tag{4}$$

where $Z^{TS}$ and $Z^R$ are the partition functions of the transition state and the reactant, respectively.

If there are many degrees of freedom affecting the transfer, direct evaluation of the extremal instanton trajectory is not feasible and therefore approximations are necessary. Based on exact instanton solutions for two- and three-dimensional models, we have developed an approximation scheme for the instanton action $S_I(T)$ whereby direct evaluation of the instanton trajectory is avoided. First, the multidimensional potential-energy surface is generated in a form suitable for the instanton calculations. It is derived from *ab initio* calculations of the structure, energy, and force field of the initial, final, and transition state, and formulated in terms of the normal modes of the transition state. The mode $x$ with imaginary frequency is the reaction coordinate and the remaining transverse modes **y** are treated as independent harmonic oscillators coupled linearly to $x$. Then the required coupling constants are derived from the displacements of the modes between the stable configurations and the transition state. This coupling can enhance or suppress tunneling, depending on whether the coupled mode is (approximately) symmetric ($s$) or antisymmetric ($a$) relative to the reaction coordinate. Antisymmetric coupling contributes effectively to the Franck–Condon factor of the transition (or friction) and thus lowers the rate. Symmetric coupling facilitates the transfer through the lowering of the effective barrier height and width. The instanton action in Eq. (3) is found to assume the form

$$S_I(T)=\frac{S_I^0(T)}{1+\Sigma_s\delta_s(T)}+\alpha_s\sum_a\ \delta_a(T), \tag{5}$$

and the proportionality factor $A(T)$ is approximated by

$$A(T)=\Omega_0/2\pi, \tag{6}$$

$\Omega_0$ being the effective frequency of the reaction coordinate in the initial state. In Eq. (5) $S_I^0(T)$ is the one-dimensional instanton action evaluated with the vibrationally adiabatic potential along the reaction coordinate and the renormalized (dimensionless) coordinate-dependent mass of tunneling $m_{\mathrm{eff}}(x)\geqslant 1$. It accounts for the coupling to modes that are faster than the tunneling motion under the barrier. The slower modes contribute via the corrections $\delta_{a,s}(T)$ and the factor $\alpha_s<1$ describes the modulation of the Franck–Condon factor by tunneling-enhancing modes. The effective parameters $\Omega_0$ and $m_{\mathrm{eff}}(x)$ and the corrections $\delta_{a,s}(T)$ are expressed analytically in terms of the normal mode frequencies and displacements, and the evaluation of $S_I^0(T)$ for a given temperature is performed through a simple numerical integration.[1,2]

## III. GAS-PHASE CALCULATIONS

The level of theory adopted for the calculations of the 1:1 and 1:2 complexes of $7AI/S_1$ with water is the complete active space multiconfiguration self-consistent-field (CASSCF)[19] method with a 6-31G* basis set. The active space includes the four occupied $\pi$ orbitals of highest energy and the four unoccupied $\pi^*$ orbitals of lowest energy, referred to as CASSCF(8,8)/6-31G* hereafter. Optimized structures and energies are calculated for the (meta)stable configurations and the transition states. The principal results are listed in Table I and depicted in Figs. 1 and 2.

TABLE I. Relative energies (in kcal/mol) and dipole moments (in D) for all the complexes studied.

| | | CASSCF/6-31G* | | CASSCF/6-31G*/Onsager | |
|---|---|---|---|---|---|
| | | Relative energy | Dipole moment | Relative energy | Dipole moment |
| $7IA\cdot H_2O$ | **N-1** | 0.00 | 1.99 | 0.00 | 2.47 |
| | **TS-1** | 20.64 | 5.02 | 17.94 | 6.50 |
| | **T-1** | −33.19 | 2.06 | −33.37 | 2.56 |
| $7IA\cdot 2H_2O$ | **N-2c** | 0.00 | 1.51 | 0.00 | 2.07 |
| | **TS-2c** | 16.94 | 6.88 | 11.61 | 9.05 |
| | **T-2c** | −32.45 | 2.21 | −32.83 | 3.19 |
| | **N-2n** | 6.32 | 2.35 | 5.60 | 3.94 |
| | **TS-2n** | 19.83 | 2.49 | 18.68 | 4.95 |
| | **T-2n** | −27.06 | 2.39 | −27.85 | 4.02 |
| $7IA\cdot 5H_2O$ | **N-2(3)c** | 0.00 | 2.51 | 0.00[a] | 2.85 |
| | **TS1-2(3)c** | 7.62 | 4.80 | 6.63 | 5.35 |
| | **IP-2(3)c** | 5.80 | 6.08 | 2.97 | 7.03 |
| | **TS2-2(3)c** | 5.81 | 5.75 | 3.67 | 6.55 |
| | **T-2(3)c** | −32.85 | 2.82 | −32.61 | 3.09 |
| | **N-1(4)** | 1.08 | 1.31 | 1.43 | 1.54 |
| | **TS-1(4)** | 19.00 | 5.13 | 17.39 | 5.86 |
| | **T-1(4)** | −32.09 | 1.54 | −31.77 | 1.71 |

[a]Single-point calculations using the CASSCF(8,8)/6-31G* optimized geometry.

The listed values for the 1:1 complex are in good agreement with the CASSCF(9,10)/DZP results reported by Chaban and Gordon.[12] As shown in Fig. 1, the two hydrogen bonds are nonlinear in the triangular NHOHN arrangement and therefore subject to strain. As a result these bonds are unequal in the metastable canonical form **N-1** but almost equal in the tautomeric form **T-1** that is the stable configuration in the excited state. In the transition state **TS-1** the hydrogen bonds are considerably shorter and their added strength is seen to distort the 7AI skeleton. As expected[1,2] on the basis of the large exothermicity, listed in Table I, the two protons move asynchronously, the water proton moving towards $N_7$ before the $N_1$ proton moves to O.

For the 1:2 complex we have found two conformers. In the cyclic 1:2 complex, **N-2c**, shown in Fig. 2, which is the lowest-energy excited **N**-type conformer found for this complex, the hydrogen-bonding pattern is different from that in the 1:1 complex due to the absence of strain in the square NHOHOHN structure. The NH···O and N···HO hydrogen bonds are almost equal in both the **N-2c** and the **T-2c** configuration. The alternative noncyclic conformer, **N-2n**, depicted also in Fig. 2, amounts to a 1:1 complex microsolvated by a single water molecule hydrogen-bonded to the water bridge. Its energy is about 6 kcal/mol higher than that of the cyclic conformer.

Correspondingly, two transition states have been found, depicted as **TS-2c** and **TS-2n** in Fig. 2. **TS-2c** corresponds to a basically planar cyclic structure with shortened hydrogen bonds relative to **N-2c**. The strengthening of the hydrogen bonds in this transition state does not give rise to a significant distortion of the 7AI skeleton, although it reduces the barrier height by almost 4 kcal/mol relative to the 1:1 com-

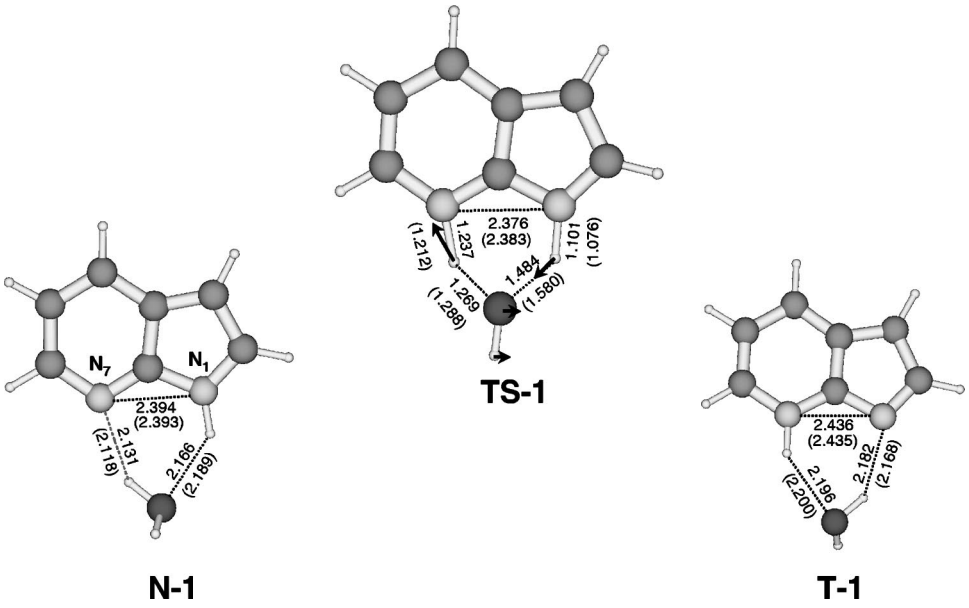


FIG. 1. Calculated structures of the stationary points along the reaction coordinate for the **N**→**T** transition in excited 7-azaindole·$H_2O$. The distances in Å refer to calculations at the CASSCF(8,8)/6-31G* level. Numbers in parentheses refer to structures reoptimized in an Onsager cavity.

plex. On the other hand, proton transfer, again initiated by transfer of a water proton to $N_7$, is much more asynchronous than in the 1:1 complex. It is accompanied by a displacement of the two solvent molecules, which allows them to share the partial charge generated by the proton motion. As a result of this double oxygen motion, the imaginary frequency of **TS-2c** is much smaller than that of **TS-1**, and the barrier is much lower due to the resulting stabilization of the polar structure, as shown in Table I. The alternative transition state **TS-2n**, on the other hand, remains much closer to **TS-1**. It is indeed characterized by a single-molecule water bridge, similar to that of the 1:1 complex microsolvated by one water molecule that is hydrogen-bonded to $N_7$. Comparison with **TS-1** shows that this hydrogen bond shifts the bridging water molecule towards $N_1$, resulting in a more asynchronic transfer mechanism characterized by a larger effective mass and a lower imaginary frequency: 1269*i* vs 1749*i* $cm^{-1}$. Both structurally and energetically, the noncyclic 1:2 complex is intermediate between the 1:1 complex and the cyclic 1:2 complex, but much closer to the former. Therefore we focus henceforth on the 1:1 and cyclic 1:2 complexes.

In Tables II and III we list the coupling parameters between the reaction coordinate and the symmetric and antisymmetric components of the transverse modes and the effective mass as a function of the reaction coordinate for the 1:1 and 1:2 complexes, respectively. We also list the tunnel-

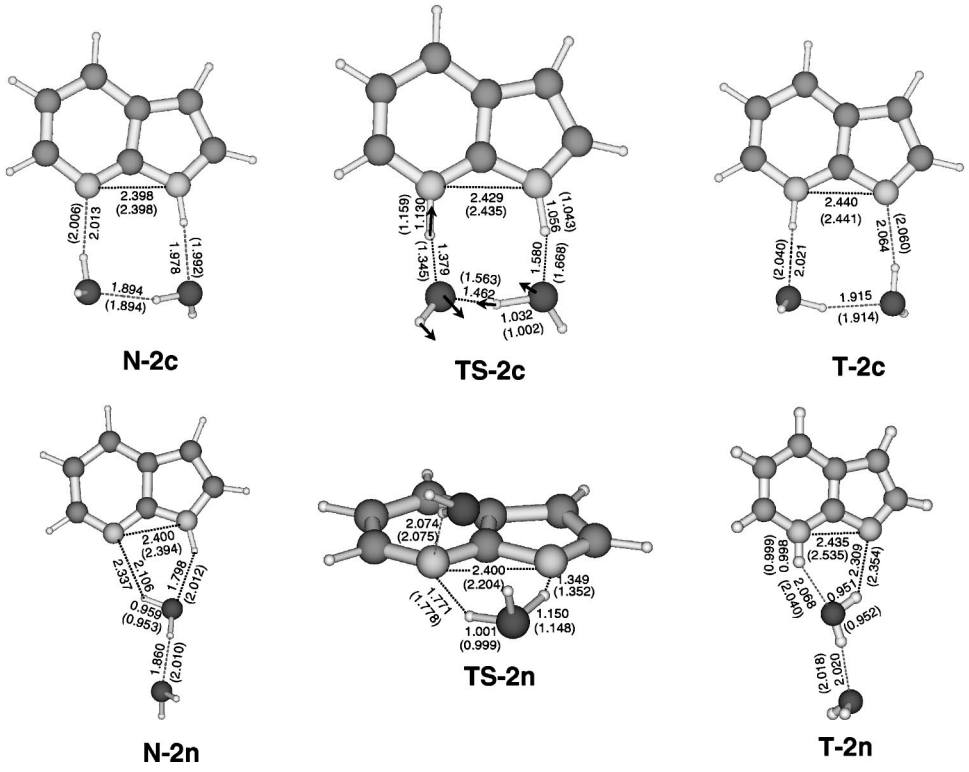


FIG. 2. Same as Fig. 1 for excited 7-azaindole·$(H_2O)_2$.

TABLE II. Major dynamics parameters and rate constants (in $s^{-1}$) for the 1:1 complex.

| | CASSCF/6-31G* | CASSCF/6-31G*/Onsager |
|---|---|---|
| Vibrational adiabatic barrier height (kcal/mol) | 22.07 | 19.28 |
| Imaginary frequency ($cm^{-1}$) | 1749 | 1749[a] |
| Effective frequency in the well of **N-1**, $\Omega_0$ ($cm^{-1}$) | 3131 | 3131[a] |
| Tunneling distance (A $amu^{1/2}$) | 1.621 | 1.631 |
| Parameter of enhancing coupling $\delta_s$ | 0.245 | 0.321 |
| Parameter of suppressing coupling $\delta_a$ | 3.166 | 1.920 |
| Effective mass of tunneling $m_{\text{eff}}(x)$ | $2.3x^2+0.2$ | $2.2x^2+0.2$ |
| $k_{\text{tun}}$ ($T=0$ K) | $9.7\times10^{1}$ | |
| $k_{\text{tun}}$ ($T=300$ K) | $1.6\times10^{4}$ | $9.9\times10^{5}$ |
| $k_{\text{cl}}$ ($T=300$ K) | $6.3\times10^{-2}$ | 6.8 |

[a]Same as for the CASSCF/6-31G* level.

ing rate constants of Eq. (3) at 0 and 300 K calculated from Eqs. (6) and (7) along with the classical rate constants of Eq. (4) calculated by conventional transition-state theory.[18]

It follows from Tables II and III that in all these complexes the tautomerization occurs by quantum-mechanical tunneling, the classical contributions to the rate constants being negligible or small. As indicated by Fig. 1, the process of double proton transfer in the 1:1 complex is not synchronous, but the contribution of heavy-atom motions remains limited. This follows from the high value of the imaginary frequency ($1749i$ $cm^{-1}$), which indicates predominant hydrogenic motion, as depicted in Fig. 1. The low-temperature rate constants are well below the upper limit set by the cold-beam experiments. The increase of the rate constant with temperature is much too slow to account for the observed transfer rate in aqueous solution.

The triple proton transfer in the cyclic 1:2 complex is accompanied by strong reorganization of the heavy atoms, illustrated in Fig. 2 by the substantial change of the square NHOHOHN structure between the **N-2c** and **TS-2c** configurations. This leads to a larger effective mass of tunneling, reflected in the low value of the imaginary frequency ($511i$ $cm^{-1}$) of the normal mode shown in Fig. 2. The results for the 1:1 and cyclic 1:2 complexes, listed in Tables II and III show the balance between the positive effects of the lower barrier and shorter tunneling distance, and the negative effects of the larger effective mass and weaker coupling to symmetric (helping) modes. The negative effects turn out to be dominant in the tunneling region, but the positive effects dominate in the classical (high-temperature) region. The parameters of the noncyclic 1:2 complex, not listed in Table III, correspond to a purely classical mechanism with a rate much lower than that of the cyclic complex. Thus for all 1:1 and 1:2 gas-phase complexes the calculated rate constants are in agreement with the observed absence of tautomerization in cold beams.

These results shed no direct light on the very high transfer rates in protic solutions, although they suggest substantial charge separation in the transition states, especially of the cyclic 1:2 complex, which may give rise to a large solvent effect. This aspect we explore in the next section.

## IV. CALCULATIONS IN SOLUTION

To simulate the effect of solvation on the complexes we use two methods. The first method is based on the self-consistent reaction field/Onsager model[14] as implemented in GAUSSIAN 98.[15] We embed the complex in a spherical cavity inside a dielectric continuum with the dielectric constant of bulk water. We reoptimize the geometries at the CASSCF(8,8)/6-31G*/Onsager level, the results of which are shown in parentheses in Figs. 1 and 2. The pertinent parameters obtained by using these geometries in conjunction with the gas phase force fields are listed in Tables II and III, where they are compared with the corresponding parameters for the isolated complexes.

The results show that this form of solvation has no significant effect on the geometries of the (meta)stable configurations (**N** and **T**), whose relative stability remains almost unchanged. It has a larger effect on the transition states (**TS**)

TABLE III. Same as Table I for the 1:2 cyclic complex.

| | CASSCF/6-31G* | CASSCF/6-31G*/Onsager |
|---|---|---|
| Vibrationally adiabatic barrier height (kcal/mol) | 17.11 | 11.77 |
| Imaginary frequency ($cm^{-1}$) | 511 | 511[a] |
| Effective frequency in the well of **N-2c**, $\Omega_0$ ($cm^{-1}$) | 1780 | 1780[a] |
| Tunneling distance (A $amu^{1/2}$) | 1.002 | 1.099 |
| Parameter of enhancing coupling $\delta_s$ | 0.004 | 0.000 |
| Parameter of suppressing coupling $\delta_a$ | 3.015 | 3.045 |
| Effective mass of tunneling $m_{\text{eff}}$ | $4.4\times10^{2}x^2+6.3$ | $3.9\times10^{4}x^2+56.7$ |
| $k_{\text{tun}}$ ($T=0$ K) | $6.4\times10^{-10}$ | |
| $k_{\text{tun}}$ ($T=300$ K) | $8.0\times10^{1}$ | $9.8\times10^{4}$ |
| $k_{\text{cl}}$ ($T=300$ K) | 5.3 | $4.1\times10^{4}$ |

[a]Same as for the CASSCF/6-31G* level.

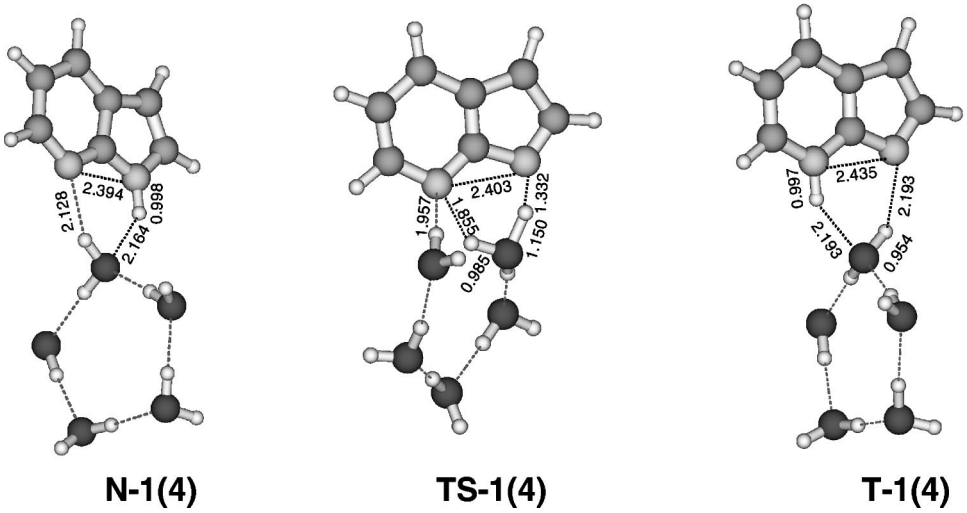


FIG. 3. Same as Fig. 1 for excited 7-azaindole$\cdot(H_2O)_{1+4}$.

because the transition states are more polar as follows from their dipole moments. For instance, the dipole moments of the **N-1** and **TS-1** forms in solution are 1.5 D and 6.9 D while those of the **N-2c** and **TS-2c** forms are 2.1 D and 9.1 D, respectively. Specifically the larger charge separation in the transition state of the cyclic 1:2 complex relative to the 1:1 complex is reflected in the stronger reduction of the barrier height. Correspondingly, the changes in geometry upon solvation, shown in Figs. 1 and 2, indicate an enhancement of the ionic character of the transition states. The bulk solvent effect increases the double proton transfer rate constant in the 1:1 complex by a factor of about 60, as shown in Table II. In the cyclic 1:2 complex the increase in the triple proton transfer rate constant is much larger, but still far from enough to account for the observed rate constants in protic solution. Evidently, the continuum model does not account properly for the effect of additional solvent molecules on these complexes.

We therefore consider an alternative method to simulate the effect of solvation, namely the addition of discrete water molecules to form a secondary solvent shell. Obviously, the present level of theory imposes severe limitations on the number of additional molecules that can be handled with the required accuracy. We therefore restrict ourselves to two 1:5 complexes corresponding to **N-1** with four and **N-2c** with three additional solvent molecules, which complexes we denote by **N-1(4)** and **N-2(3)c**, respectively. The chosen structures for these complexes, illustrated in Figs. 3 and 4, respectively, are obtained by optimizing configurations with the maximum number of linear hydrogen bonds associated with the secondary shell.

The structure of these complexes in their stable configurations and in the transition states for proton transfer are optimized at the CASSCF(8,8)/6-31G* level. The pertinent dimensions are given in Figs. 3 and 4. Based on the results obtained for the 1:1 and 1:2 complexes, we expect embedding the 1:5 complexes in a dielectric continuum to have only a minor effect on the structure. Since optimization at the CASSCF(8,8)/6-31G*/Onsager level is very laborious for these large complexes, we therefore carried out single-point Onsager calculations at the stationary CASSCF(8,8)/6-31G* geometries. The relevant parameter values are collected in Table I.

The effect of the discrete second solvent shell on the structure in the proton-transfer region is very different for the two complexes, as shown by the data in Table I. For the **N-1(4)** complex the principal effect of the secondary shell is a modest reduction of the proton transfer barrier, comparable to the effect of the dielectric continuum on the barrier height of **N-1**. Single-point Onsager calculations at the CASSCF geometry of **TS-1(4)** have little effect on the barrier height. For **N-2(3)c**, however, the reduction in barrier height relative to **N-2c** is drastic enough to produce a (meta)stable intermediate state, to be denoted by **IP-2(3)c**. Here the reduction is more than twice that effected by the dielectric continuum. Moreover, unlike the dielectric continuum, the three molecules forming the secondary shell also have a major effect on the structure of this complex. They redistribute the strength of the three primary hydrogen bonds in the **N** and **T** configurations without, however, changing the exothermicity significantly, the overall polarity being very similar in these configurations. For the **IP-2(3)c** structure the energy is reduced to a value similar to that for **TS2-2(3)c**. A further reduction of its energy is obtained if the **N-2(3)c** complex is immersed in a dielectric continuum, as indicated by the results of single-point Onsager calculations at the CASSCF geometries, which produce an ion-pair minimum, separated from the **N-2(3)c** and **T-2(3)c** configurations by barriers of 3.67 and 0.71 kcal/mol, respectively. The latter barrier may be too small to support a bound state in this minimum.

From the calculated barrier heights of the single- and double-bridged 1:5 complexes, it follows immediately that the latter will tautomerize much more rapidly. Because the available computational facilities make it impossible to use CASSCF(8,8)/6-31G* level calculations to obtain the vibrational force field required for a quantitative evaluation of the dynamics at this level of theory, we use a dual-level dynamics approach. An analogous stategy is used in transition-state theory with tunneling corrections, where it is common practice to use semiempirical methods to interpolate between *ab initio* results. In the present case, the use of a more approximate method should be adequate for the semiquantitative

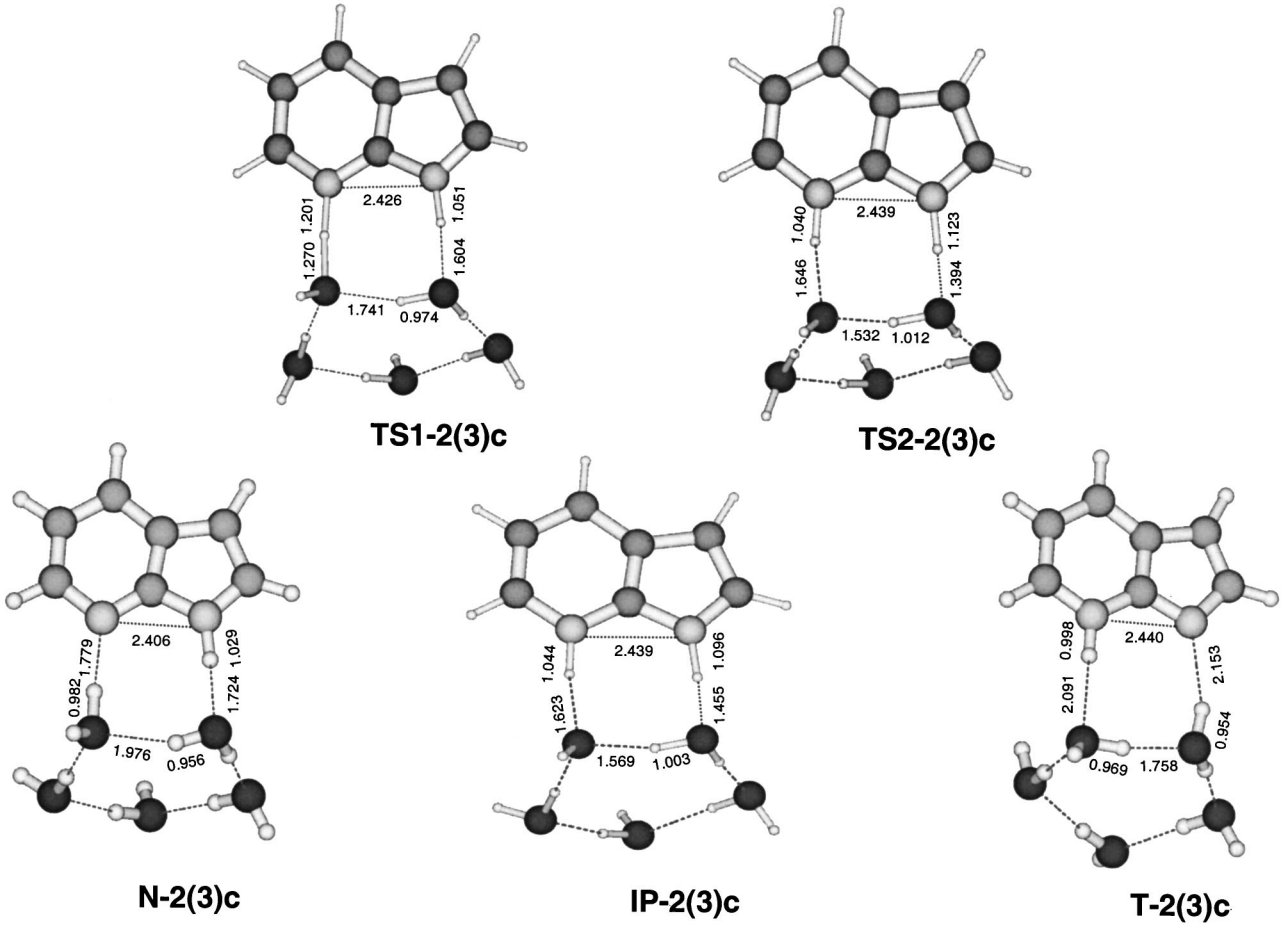


FIG. 4. Same as Fig. 1 for excited 7-azaindole$\cdot(H_2O)_{2+3}$.

purpose of comparing the transfer rates in single- and double-bridged complexes. As in Ref. 1, we combine the geometries and frequencies of the stationary points at the CIS/6-31G level with the energetics of the CASSCF(8,8)/6-31G*/Onsager level. The CIS/6-31G level is chosen because it approximately reproduces the pertinent relative energies obtained at the CASSCF level in the neighborhood of the central well of **TS-2(3)c**; specifically the energy differences of **TS1-2(3)c** and **TS2-2(3)c** with **IP-2(3)c** are 4.65 and 0.44 kcal/mol at the CIS level, and 3.67 and 0.71 kcal/mol at the CASSCF level. Using this approach we can calculate the rate of concerted double proton tunneling in the single-bridged 1:5 complex by the DOIT 1.2 code in a straightforward manner. The value at room temperature is about 2 $s^{-1}$, so that this process can be ruled out as a significant contributor to the fast tautomerization component.

An analogous calculation of the rate constant for the process **N-2(3)c**→**T-2(3)c** is not possible because of the complicated shape of the potential. However, since the reported experimental values are only order-of-magnitude results, it is still relevant to compare them with rough theoretical estimates. If we take the CASSCF(8,8)/6-31G*/Onsager energies in Table I at face value and assume that there is no bound state in the central well, we can easily calculate the classical contribution to the rate constant at 300 K. The result is $k_{\mathrm{cl}}(300)=3\times10^{8}$ $s^{-1}$, a value that approaches the observed maximum rate constant from below. There will be a tunneling contribution as well, but it is not immediately clear how to define the reaction coordinate for a central well without a bound state. If a bound state were present, the rate-determining first step **N-2(3)c**→**IP-2(3)c** would yield a rate constant $k_{\mathrm{tun}}(300)=8\times10^{10}$ $s^{-1}$, a value that approaches the observed maximum rate constant from above. These two rough estimates of the classical and tunneling transfer rate constants, calculated with the parameters listed in Table IV, bracket the experimental estimate and make it plausible that the fast tautomerization process observed in protic solvents involves solvated 1:2 complexes of 7AI. Whether the leading component is concerted or stepwise, and governed by tunneling or classical transfer cannot be established with confidence at the present level of theory.

## V. DISCUSSION

From the observation that tautomerization of excited 7AI is catalyzed by protic solvents, it has been generally concluded that a solvent molecule such as water or an alcohol forms a bridge that acts as a pathway for double proton transfer. Although this process has generated wide interest, the present calculations represent the first attempt to calculate the rate of such a process from first principles. Rate constant calculations for isolated small complexes of 7AI with water are relatively straightforward, as shown by our earlier calculations of $7AI/S_0$ complexes,[1] for which, however, no experi-

TABLE IV. Major dynamics parameters for the reaction **IP-2(3)c→N-2(3)c** under the assumption that there is a bound state in **IP-2(3)c**. The **N2(3)c→IP-2(3)c** rate constants (in $s^{-1}$) listed in the table are obtained from microscopic reversibility.

| | Dual-level calculations[a] |
|---|---|
| Vibrational adiabatic barrier height (kcal/mol) | 4.03 |
| Imaginary frequency ($cm^{-1}$) | 833 |
| Effective frequency in the well of **IP2(3)c**, $\Omega_0$ ($cm^{-1}$) | 1402 |
| Tunneling distance (A $amu^{1/2}$) | 0.684 |
| Parameter of enhancing coupling $\delta_s$ | 0.135 |
| Parameter of suppressing coupling $\delta_a$ | 3.166 |
| Effective mass of tunneling $m_{\text{eff}}(x)$ | $2.3\times10^{1}x^{2}+0.1$ |
| $k_{\text{tun}}$ ($T=300$ K) | $8.2\times10^{10}$ |
| $k_{\text{cl}}$ ($T=300$ K) | $2.9\times10^{8}$ |

[a]Combining the geometries and frequencies of the stationary points at the CIS/6-31G level with the energetics of the CASSCF(8,8)/6-31G*/Onsager level.

mental rate data are available. For complexes of $7AI/S_1$ with one or two water molecules an upper limit of about $10^7$ $s^{-1}$ can be deduced from the observation that in cold beams they show no tautomerization within the fluorescence lifetime of 8 ns. The results of the calculations listed in Tables II and III agree with these observations and indicate that the concerted two-proton tunneling rate constants, which dominate the tautomerization, are well below this limit. The calculations also yield room-temperature rate constants which are very much lower than the maximum rate constants measured in dilute solutions in water and alcohols, which amount to about $10^{10}$ $s^{-1}$. The gap between the observed and calculated rate constants cannot be bridged by the Onsager model, which treats the bulk solvent as a dielectric continuum around a spherical cavity occupied by the complex and leads to tunneling rate constants of $10^5-10^6$ $s^{-1}$. This indicates the need for a more detailed treatment of the solvation of the complexes.

Since protic solvents form hydrogen-bonded networks, the treatment chosen is microsolvation of the 1:1 and 1:2 complexes by discrete water molecules arranged to form such a network. To keep the calculations tractable, the total number of water molecules is limited to five, which is sufficient to yield essentially unstrained hydrogen bonds. The resulting 1:5 complexes are again embedded in a dielectric continuum according to the Onsager model. In this case the dynamics calculations are not straightforward, the complexity of the systems requiring a number of simplifications in the calculations. The results, however, are unambiguous: Rate constants for 1:2 complexes microsolvated by three water molecules are very much larger than those for 1:1 complexes microsolvated by four water molecules, in sharp contrast to the rate constants for the isolated complexes. The main reason for this change is that in the 1:2 complex there is enough charge separation to replace the barrier by a central well upon microsolvation, whereas in the 1:1 complex the charge separation is small so that microsolvation has a minimal effect on the barrier. As a result proton transfer in the 1:(2+3) complex begins to approach a classical two-step process, although according to our best estimate one-proton tunneling will win out as the rate-determining first step by a modest margin; for the 1:(1+4) complex, on the other hand concerted triple proton tunneling remains strongly dominant. Comparison with experiment indicates that the rate constants calculated for the microsolvated 1:2 complex are of the same order of magnitude as the fast component observed in solution, while those for the microsolvated 1:1 complex are too small to contribute significantly to the tautomerization in solution.

To support this unconventional result we note that, given the abundance of solvent molecules, it is *a priori* highly probable that in dilute solutions the two nitrogen atoms of 7AI are solvated by different water molecules. Moreover, such structures tend to have lower energies than equivalent structures with a single bridging water molecule where the hydrogen bonding is necessarily strained. If the two nitrogen atoms are bound to different water molecules, proton transfer will be blocked unless these water molecules are directly or indirectly connected by hydrogen bridges. The rapid interchange between unstrained and thus roughly isoenergetic hydrogen-bonded networks, leading intermittently to suitably short bridges for proton transfer, offers a rationalization for the observed kinetic complexity of the tautomerization of $7AI/S_1$ in aqueous solution.

[1] Z. Smedarchina, W. Siebrand, A. Fernández-Ramos, L. Gorb, and J. Leszczynski, J. Chem. Phys. **112**, 566 (2000).
[2] A. Fernández-Ramos, Z. Smedarchina, and M. Z. Zgierski, J. Chem. Phys. **113**, 2662 (2000).
[3] A. Nakajima, F. Ono, Y. Kihara, A. Ogawa, K. Matsubara, K. Ishikawa, M. Baba, and K. Kaya, Laser Chem. **15**, 167 (1995).
[4] Y. Huang, S. Arnold, and M. Sulkes, J. Phys. Chem. **100**, 4734 (1996).
[5] A. Nakajima, M. Hirano, R. Hasumi, K. Kaja, H. Watanabe, C. C. Carter, J. M. Williamson, and T. A. Miller, J. Phys. Chem. A **101**, 392 (1997).
[6] D. McMorrow and T. J. Aartsma, Chem. Phys. Lett. **125**, 581 (1986).
[7] R. S. Moog and M. Maroncelli, J. Phys. Chem. **95**, 10359 (1991).
[8] C. F. Chapman and M. Maroncelli, J. Phys. Chem. **96**, 8430 (1992).
[9] Y. Chen, R. L. Rich, F. Gai, and J. W. Petrich, J. Phys. Chem. **97**, 1770 (1993).
[10] S. Mente and M. Maroncelli, J. Phys. Chem. A **102**, 3860 (1998).
[11] M. S. Gordon, J. Phys. Chem. **100**, 3974 (1996).
[12] G. M. Chaban and M. S. Gordon, J. Phys. Chem. A **103**, 185 (1999).
[13] A. Fernández-Ramos, Z. Smedarchina, W. Siebrand, M. Z. Zgierski, and M. A. Rios, J. Am. Chem. Soc. **121**, 6280 (1999).
[14] L. Onsager, J. Am. Chem. Soc. **58**, 1486 (1963); M. W. Wong, K. B. Wiberg, and M. J. Frisch, J. Chem. Phys. **95**, 8991 (1991); M. W. Wong, M. J. Frisch, and K. B. Wiberg, J. Am. Chem. Soc. **113**, 4776 (1991).
[15] M. J. Frisch, G. W. Trucks, H. B. Schlegel *et al.*, GAUSSIAN 98, Revision A.3, Gaussian Inc., Pittsburgh, PA, 1998.

[16] M. W. Schmidt, K. K. Baldridge, J. A. Boatz, S. T. Elbert, M. S. Gordon, J. H. Jensen, S. Koseki, N. Natsunaga, K. A. Nguyen, S. J. Su, T. L.Windus, M. Dupuis, and J. A. Montgomery, J. Comput. Chem. **14**, 1347 (1993).
[17] Z. Smedarchina, A. Fernández-Ramos, W. Siebrand, and M. Z. Zgierski, DOIT 1.2, a computer program to calculate hydrogen tunneling rate constants and splittings, National Research Council of Canada (2000) (http://gold.sao.nrc.ca/sims/software/doit1.2/index.html).
[18] K. J. Laidler, *Chemical Kinetics* (Harper & Row, New York, 1987).
[19] D. Hegarty and M. Robb, Mol. Phys. **38**, 1795 (1979).